

Study of the energy resolution in the electromagnetic end-caps of the future LDC detector for the ILC

J.Y. Hostachy¹

*Laboratoire de Physique Subatomique et de Cosmologie (LPSC),
Université Joseph Fourier, IN2P3-CNRS, F-38026 Grenoble,
France.*

M. Krim et D. Benchekroun

*Université Hassan II, Faculté des Sciences Aïn Chock, Casablanca,
Morocco.*

Abstract

The electromagnetic end-caps of the futur LDC detector for the ILC ("International Linear Collider") have been simulated with the software MOKKA [1]. The goal of this study is to determine the energy resolution with the classical method, i.e. the energy deposited in 30 + 10 active silicon layers, preceded by 1.4 and 4.2 mm of tungsten placed perpendicularly to the beam axis, respectively. The energy resolution has been fitted by the function $\Delta E/E = a/\sqrt{E} \oplus c$ and it was found that $a = 12,69 \pm 0.17 \% GeV^{1/2}$ and $c = 0.839 \pm 0.026 \%$ for incident electrons at $\theta=21,80$ degrees and $a = 13.33 \pm 0.24 \% GeV^{1/2}$ and $c = 0.968 \pm 0.050 \%$ for incident photons with the same polar angle.

¹Corresponding author, e-mail: hostachy@lpsc.in2p3.fr

1 Introduction

The following study has been performed with the help of the software MOKKA [1]. The end-caps (and the barrel) of the electromagnetic (E.M.) calorimeter are described by the system called "ecal04". In this version the end-caps are composed of 40 active silicon layers, 500 μm thick, centered at $z=2834,75$ mm for the first one, and at $z=3014,85$ mm for the last one. Each detection cell covers a surface of 10×10 mm². The first 30 active layers are preceded by 1,4 mm of tungsten (W) and the last 10 by $3 \times 1,4 = 4,2$ mm of W. One can notice that for a trajectory parallel to the beam axis, the radiation length due only to the tungsten is about $(42+42)/3,5 = 24 X_0$.

For each point, about 1000 identical particles (usually electrons) are sent into the end-caps. For each particle MOKKA creates an ASCII file (ecalNNNNNN.hits) in which all the history of the event (hit cells, energy deposits) is "mapped". All these files are read out by a C++ program which sums some of the variables and thus drastically reduces their number. The data file (corresponding to the previous 1000 files) is then analyzed by the ROOT software from CERN. To perform this analysis a set of ROOT macros have been written in C++.

The whole LDC detector has been also simulated by the MOKKA version: "D11". This version allows to introduced other sub-detectors and some of them (e.g. VXD and TPC) are located upstream from the end-caps. The presence of these sub-detectors deteriorates the energy resolution obtained from the end-caps alone.

2 Study of the energy resolution

2.1 Study of the energy resolution with the calorimeter alone

This study, where only the electromagnetic calorimeter has been taken into account, has been carried out with electrons at various energies: 5, 10, 20, 50, 100, 150, 200, 300 and 500 GeV. The direction of the electrons is represented by the vector (0 ; 0.4 ; 1) leading to an impact on the first silicon layer given by the position (0 mm ; $0.4 \times 2834.75 = 1133.90$ mm ; 2834.75 mm), that is to say $\theta = 21,80$ degrees (see fig. 1).

The energy deduced from the electromagnetic end-cap is given by the relation:

$$E = \alpha(E_1 + \beta E_2)$$

where E_1 represents the energy deposited (in MeV) in the first compartment, i.e. in the first 30 active layers of silicon, and E_2 the energy deposited (in MeV) in the last 10 layers (compartment 2). Alpha (α) is an overall coefficient of normalization (the value of the energy E will be in particular given in GeV), and

β represents the relative weight of the 2 compartments which sample the energy deposit of the incident electron. The value of β is obtained by minimizing the energy resolution for each considered energy (see fig. 2). The RMS "Root Mean Square" of each distribution in energy is automatically calculated by the software ROOT, but each one of these distributions was also fitted with a Gaussian in the interval (± 4 RMS) and centered on the average energy. This technique then enables us to deduce the Gaussian standard deviation σ which thus represents the fluctuations of energy (see fig. 3). The lack of statistics (1000 events maximum) makes however this method a little less precise to evaluate the coefficient β than that using the RMS. Nevertheless the standard deviation directly deduced from the Gaussian is less prone to an error due for example to the thrown off center positioning of some points (squared lever arm effect).

Our results were deferred in the table 1.

Table 1: Parameters α , β and standard deviations according to the energy of the incident electrons.

E (GeV)	evt #	α	β	RMS (GeV)	σ (GeV)
5	1000	0.0334	2.8	0.281	0.262
10	1000	0.0335	3.0	0.412	0.414
20	1000	0.0337	3.0	0.628	0.615
50	1000	0.0336	3.2	1.041	1.003
100	1000	0.0337	3.2	1.678	1.686
150	1270	0.0343	3.0	2.066	1.996
200	618	0.0344	3.0	2.729	2.602
300	605	0.0345	3.0	3.398	3.228
500	686	0.0346	3.0	4.796	4.714

Figures 4 and 5 show the resolution in energy (RMS/E and σ_{gauss}/E) as a function of the electron energy E. The energy resolution was fitted by the fonction:

$$\frac{\Delta E}{E} = \frac{a}{\sqrt{E}} \oplus c$$

where ΔE represents the variables RMS and σ_{gauss} .
One obtains:

$$a = 13.10 \pm 0.17 \% GeV^{1/2}$$

$$and \quad c = 0.860 \pm 0.026 \%$$

by using the RMS, and:

$$a = 12.69 \pm 0.17 \% GeV^{1/2}$$

$$\text{and } c = 0.839 \pm 0.026 \%$$

with the Gaussian fit. Mentioned uncertainties are only statistical origin.

The presence of the constant term c can be explained by the non-uniformity (existence of inactive surfaces) of the wafers (i.e. diode matrixes). If one refers for example to the document [3], the total surface of a diode matrix with its guard rings is of $6.2 \times 6.2 \text{ mm}^2$ for $6 \times 6 \text{ mm}^2$ of active surface, leading to a detection inefficiency of 6.3 %.

It will also be noticed that for $\beta=3.0$ (this parameter could be selected constant), the value of α increases very slightly according to the energy. That is perhaps due to the losses of energy which increase when the shower grows. Figure 6 highlights that this variation is logarithmic, one obtains:

$$\alpha = 0.0328 + 6.78 \cdot 10^{-4} \times \log_{10}(E \text{ (GeV)})$$

2.2 Study of the energy resolution with the whole detector and in the presence of the magnetic field of 4 T

The preceding analysis was reiterated but while taking into account this time all the detector (D11 version in MOKKA). The presence of materials (pixels, detector of vertex, TPC) upstream from the E.M. calorimeter causes to deteriorate the energy resolution of the end-caps. We thus simulated electrons with various energies having at the beginning (center of the detector) the same direction (0 ; 0.4 ; 1) that in the preceding section, and therefore the polar angle (from the cylindrical axis of symmetry (z) of the detector) is still equal to $\theta=21.80$ degrees. Our results were carried in the table 2.

Table 2: Parameters α , β and standard deviations as a function of the electron energy.

E (GeV)	evt #	α	β	RMS (GeV)	σ (GeV)
5	1000	0.0343	2.8	0.336	0.344
10	1000	0.0339	2.6	0.538	0.511
50	735	0.0338	3.4	1.333	1.301
80	927	0.0338	3.0	1.695	1.472
100	700	0.0333	3.2	1.761	1.652
200	742	0.0340	3.0	2.713	2.643
300	704	0.0341	3.0	3.488	3.346
500	778	0.0343	3.0	5.084	5.219

Figures 7 and 8 show the resolution in energy (respectively RMS/E and σ_{gauss}/E) according to energy E of the electrons with the E.M. calorimeter alone

(blue points), and by taking of account the whole detector and the magnetic field (red points). As previously, the resolution in energy was fitted by the fonction :

$$\frac{\Delta E}{E} = \frac{a}{\sqrt{E}} \oplus c$$

where ΔE represents the variables RMS and σ_{gauss} .
One obtains:

$$a = 16.46 \pm 0.24 \% \text{ GeV}^{1/2}$$

$$\text{and } c = 0.718 \pm 0.037 \%$$

using the RMS, and:

$$a = 15.48 \pm 0.24 \% \text{ GeV}^{1/2}$$

$$\text{and } c = 0.741 \pm 0.032 \%$$

with the Gaussian fit.

For $\beta=3.0$, one notices as in the preceding section that the value of α increases very slightly according to energy (perhaps because of increasing losses). One obtains:

$$\alpha = 0.0324 + 6.94 \cdot 10^{-4} \times \log_{10}(E \text{ (GeV)})$$

2.3 Study of the energy resolution with various positions

Table 3: Parameters α , β and standard deviations for 50 GeV electrons according to the polar angle θ or the radius R on the level of the first silicon active layer of one of the E.M. end-caps.

θ (degree)	R (cm)	evt #	α	β	RMS (GeV)	σ (GeV)
11.30	56.65	1000	0.0329	3.0	1.012	0.996
16.70	85.04	1000	0.0359	2.4	1.003	1.009
21.80	113.39	648	0.0336	3.2	1.041	1.003
26.56	141.74	888	0.0327	3.2	1.001	0.998
30.96	170.08	1000	0.0348	2.6	1.0085	1.021

In this analysis, only the electromagnetic calorimeter was taken into account. Electrons of 50 GeV coming from the center of the detector are sent in one of E.M. end-caps following the directions $(0 ; i \times 0.1 ; 1)$ where $i=2,3,4,5$ and 6. Our results have been reported in table 3.

The practically constant evolution of the energy resolution was represented on the figure 9. One will note that the standard deviation tends to increase very slightly ($\sim 2\%$); however this increase is to be taken with prudence because it is located in our error bars.

2.4 Study of the energy resolution with photons

A study similar to those of sections 2.1 and 2.2 was carried out starting from photons of various energies. The photons are sent in one of E.M. end-caps according to the direction (0 ; 0.4 ; 1). Our results were carried in table 4 where only E.M. calorimeter was simulated, and in table 5 where the whole detector (including the magnetic field of 4 T) was taken into account.

Table 4: Parameters α , β and standard deviations according to the energy of photons. Only the E.M. calorimeter was simulated.

E (GeV)	evt #	α	β	RMS (GeV)	σ (GeV)
5	1000	0.0333	3.0	0.291	0.281
10	1000	0.0335	3.2	0.440	0.431
20	900	0.0333	3.4	0.673	0.679
50	888	0.0337	3.2	1.202	1.114
100	800	0.0338	3.2	1.943	1.738
200	700	0.0345	3.0	2.972	2.846
300	700	0.0346	3.0	4.073	3.923
500	600	0.0346	3.0	5.331	5.094

Table 5: Parameters α , β and standard deviations according to the photon energy. The whole detector (including the magnetic field) was taken into account.

E (GeV)	evt #	α	β	RMS (GeV)	σ (GeV)
5	1000	0.0336	3.0	0.328	0.314
10	1000	0.0338	3.0	0.454	0.448
20	1000	0.0336	3.2	0.734	0.690
50	1000	0.0338	3.2	1,297	1.211
100	698	0.0332	3.4	2,003	1.708
200	700	0.0346	3.0	3.410	2.920
300	689	0.0346	3.0	4.123	3.429
500	392	0.0346	3.0	5.437	5.005

Figure 10 shows the resolution in energy (σ_{gauss}/E) obtained with the E.M. calorimeter alone, for electrons (blue points), and for photons (red points). One obtains, with the Gaussian fit and for photons :

$$a = 13.33 \pm 0.24 \% GeV^{1/2}$$

$$and \quad c = 0.968 \pm 0.050 \%$$

In the same way, figure 11 shows the resolution in energy (σ_{gauss}/E) obtained with the whole detector (including the magnetic field) for electrons (blue points) and for photons (red points). One obtains, with the Gaussian fit and for the photons:

$$a = 14.69 \pm 0.28 \% GeV^{1/2}$$

$$and \quad c = 0.836 \pm 0.045 \%$$

One notices in the first case (E.M. calorimeter alone) that the resolution in energy obtained with photons is slightly less good than that of the electrons. In the second case (all the detector) the resolution obtained with the photons is slightly better than that of the electrons, probably because of the presence of matter upstream from the end-cap and the neutrality of the photons and their higher radiation length ($9/7$ of X_0).

2.5 Comparative study with the detector ATLAS

The series of measurements carried out at the CERN with a module of the liquid argon electromagnetic barrel (quantity of material located upstream from the detector was minimized in way to possibly be able to probe the defect of the module) lead to a resolution in energy given by the relation:

$$\frac{\sigma_E}{E} = \frac{a}{\sqrt{E}} \oplus c$$

Where $a \simeq 9.2 \pm 0.1 \% GeV^{1/2}$ and $c \simeq 0.2 \pm 0.04 \%$ in an interval in pseudo-rapidity of $0.087 < \eta < 0.54$ [2].

The values obtained in this work are higher than those which one could hastily deduce from the experimental results of ATLAS. This difference is probably due to the sampling rate characterizing each calorimeter. Indeed, let us calculate the rate :

$$R = \frac{\epsilon_{activ}/L_{rad-activ}}{\epsilon_{abs}/L_{rad-abs} + \epsilon_{activ}/L_{rad-activ}}$$

where ϵ_{activ} represents the thickness of the active layer characterized by a radiation length $L_{rad-activ}$ and ϵ_{abs} represents the thickness of the absorber characterized by a radiation length $L_{rad-abs}$.

$$R_{simul} = \frac{0.500/93.6}{1.4/3.5 + 0.500/93.6} \simeq 0.0132$$

for the first compartment of the electromagnetic calorimeter simulated in this work. (The sampling rate of the second compartment will be approximately 3 times smaller).

$$R_{ATLAS} = \frac{4.0/(140. \times \cos(\alpha))}{(1.53/5.6 + 0.4/17.6)/\cos(\alpha) + 4.0/(140. \times \cos(\alpha))} \simeq 0.0880$$

for the accordion shaped E.M. calorimeter of ATLAS. The lead plates of 1.53 mm thickness are protected by 2 stainless sheets of 0.2 mm each, and the unit is thus not perpendicular to the trajectory of the particles (α angle). The gap of liquid argon (active medium) between two successive absorbers is of 2 times 2 mm.

Consequently, one obtains :

$$R_{ATLAS}/R_{simul} \simeq 6.68$$

and thus the sampling rate of the detector ATLAS is much higher than that of the detector than we simulated. The sampling rate of our calorimeter can be increased either by decreasing the thicknesses of tungsten, but in this case one has to increase the number of active layers and thus the number of electronic channels; or by increasing the thickness of the active layer, i.e. the thickness of the epitaxial layer of silicon and consequently the biasing voltage to remain with constant electric field. It should be noted that the cost of the wafers (diode matrixes) strongly depends on the quantity of basic material, i.e. silicon.

However, the Particle Flow Analysis (PFA) leads to a paradigm: "separation and reconstruction are more important than individual energy resolution". This new technique, which can be applied here, requires a very good granularity in order to identify each primary particle and then to separate the contribution of each shower due to these particles, avoiding as much as possible overlapping.

3 Conclusion

In this note, we have, using the software of simulation MOKKA, determined the energy resolution of the E.M. end-caps for the future detector LDC of the ILC. It should be noted that the depth (1 absorber + 1 active layer) equal to 3.90 mm in MOKKA is probably slightly optimistic; (the prototypes constructed to date by the LLR lead to the following values: 1.4 mm of W + 0.500 mm of Si + 2×0.150 of carbon fibers + 2.4 mm for the PCB, i.e. ~ 4.6 mm).

The energy resolution for the end-caps of the E.M. calorimeter alone, was determined with electrons and at the radial position $R \simeq 113.4$ cm; it was found:

$$\Delta E/E = (12,69 \pm 0.17) \% / \sqrt{E(GeV)} \oplus (0.839 \pm 0.026) \%$$

For the same position, but with photons, it leads to a resolution:

$$\Delta E/E = (13.33 \pm 0.24) \%/ \sqrt{E(\text{GeV})} \oplus (0.968 \pm 0.050) \%$$

near to that obtained with electrons. However the value of these resolutions probably seems to us a little low because of the weak sampling rate which characterizes the detector.

We also determined the resolution in energy by taking of account the whole detector. Our analysis leads to the following results, for electrons :

$$\Delta E/E = (15.48 \pm 0.24) \%/ \sqrt{E(\text{GeV})} \oplus (0.741 \pm 0.032) \%$$

and for photons :

$$\Delta E/E = (14.69 \pm 0.28) \%/ \sqrt{E(\text{GeV})} \oplus (0.836 \pm 0.045) \%$$

The resolution in energy could also be estimated from the number of hitted detection cells (for example for 100 GeV electrons approximately 1000 cells are hitted). One can hope that this new method will be sufficiently precise and and not correlated to the preceding one to improve the energy resolution. This operation will be able to be done by analyzing event by event and with different weights (related to the relative accuracy of the 2 methods) the 2 predictions and to thus reach a better resolution. It will be one of the goals which we propose to reach in the future.

Acknowledgments

We would like to express our gratitude to M. Gabriel Musat from LLR-Palaiseau, who, with lots of patience, explained us how to use the software MOKKA.

This work was carried out under the International Research Group (IRG) agreement between IN2P3/CNRS, l'Université Joseph Fourier of Grenoble, l'Université de Méditerranée of Aix-Marseille II, l'Université de Savoie, the Moroccan CNRST and KTH Sweden.

References

- [1] "MOKKA - a detailed Geant4 detector simulation for the Future Linear Collider"
<http://polywww.in2p3.fr/geant4/tesla/www/mokka/mokka.html>
- [2] B. Aubert et al., Nucl. Instr. and Meth. A 500 (2003) 202.
- [3] S. Valkar et al., DESY proposal for R&D, PRC 01-02, March 2001.
http://polywww.in2p3.fr/flc/calice_offic.html

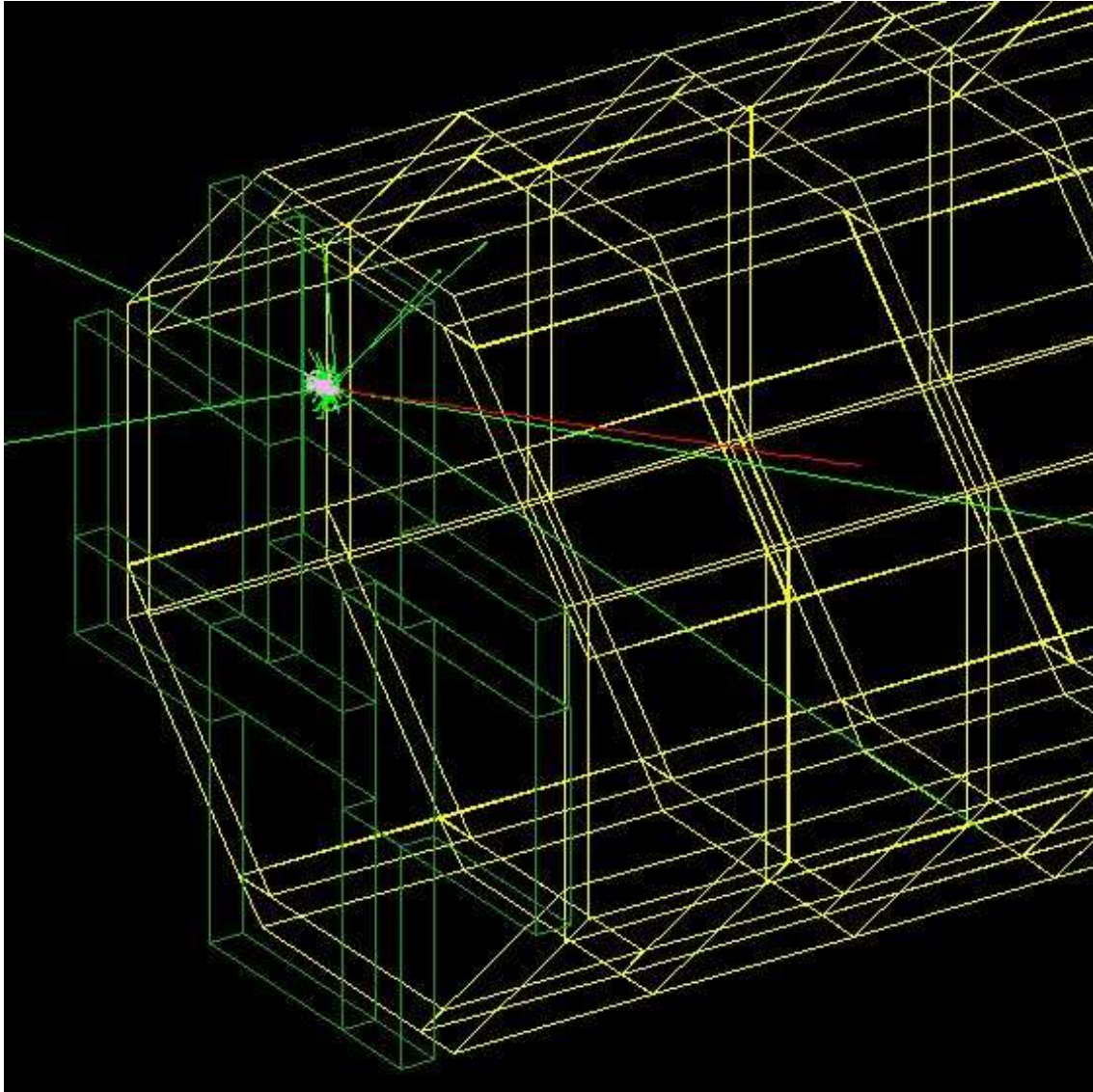


Figure 1: Shower due to an electron of 5 GeV penetrating in one of the end-caps of the electromagnetic calorimeter.

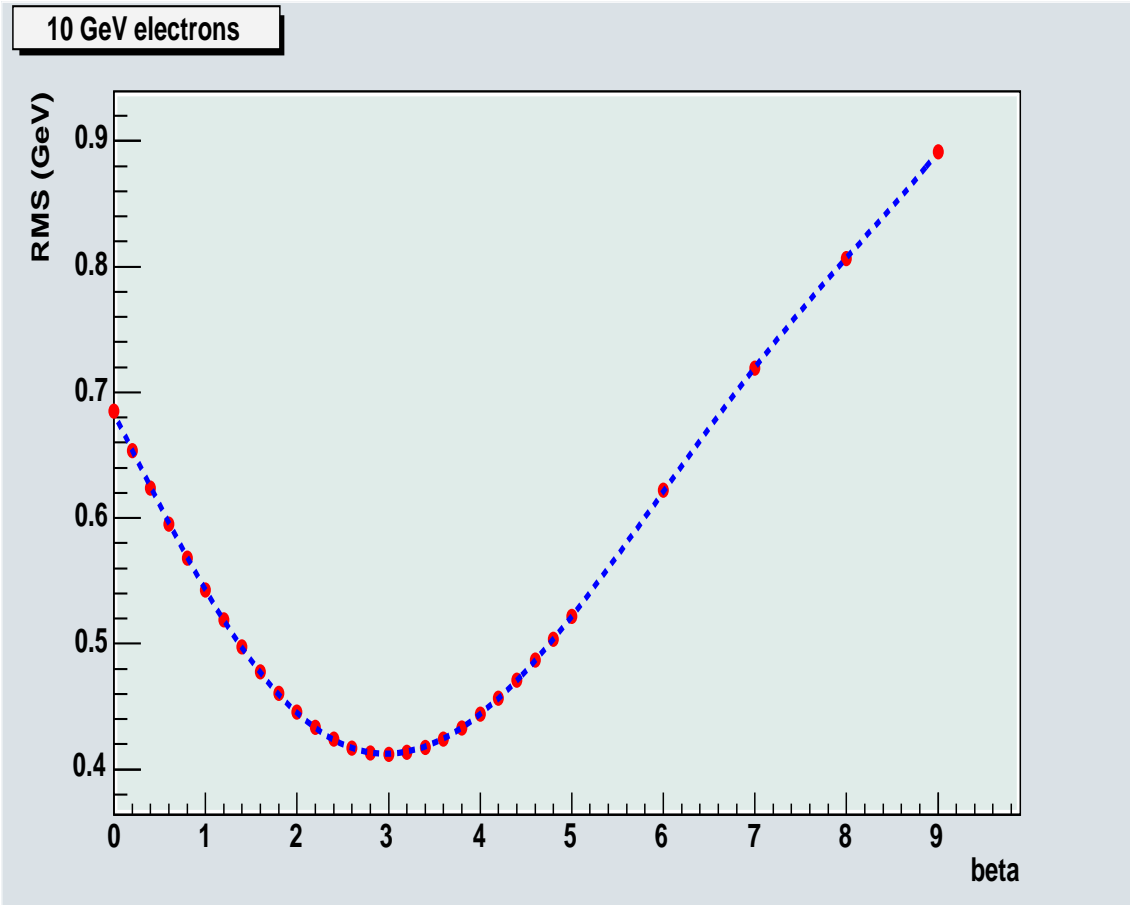


Figure 2: Standard deviation according to the weight β (see text). We plotted the curve in dotted lines in order to guide the eye.

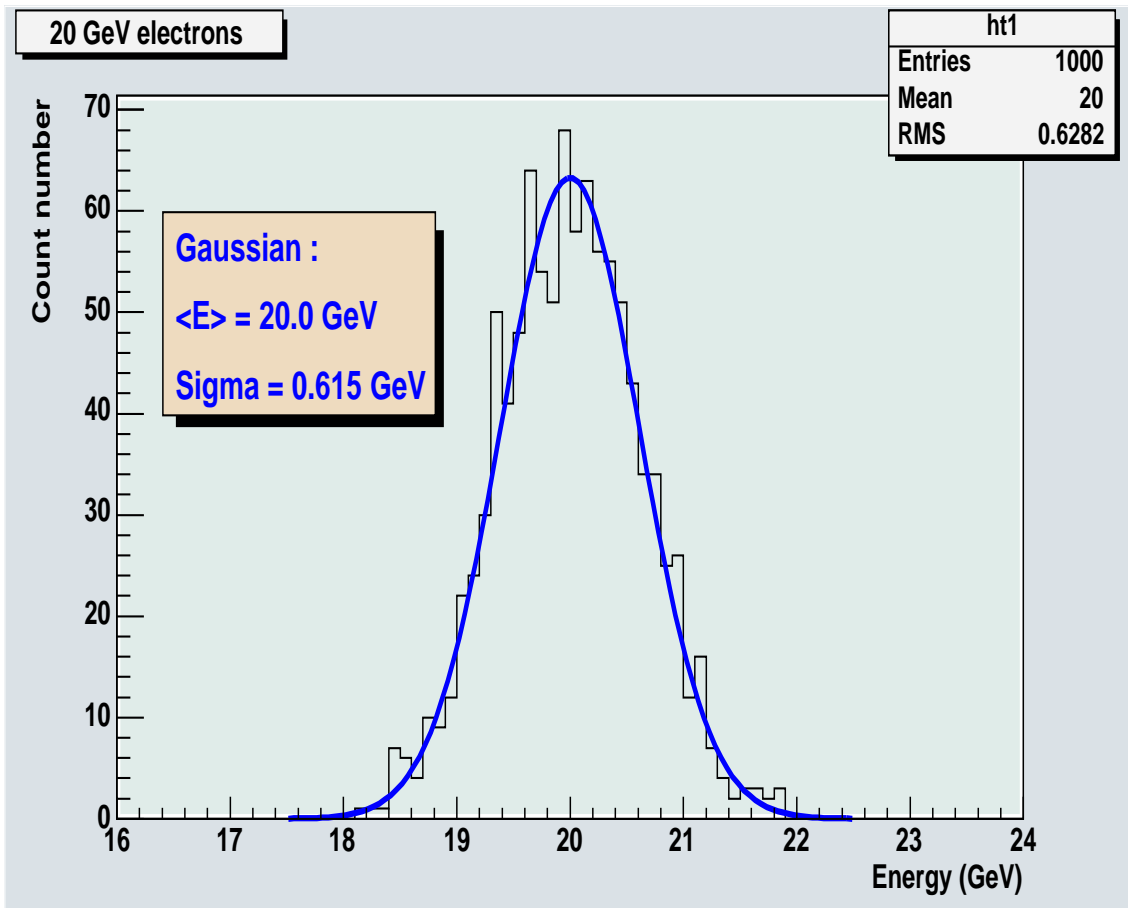


Figure 3: Energy distribution for 20 GeV electrons fitted by a Gaussian.

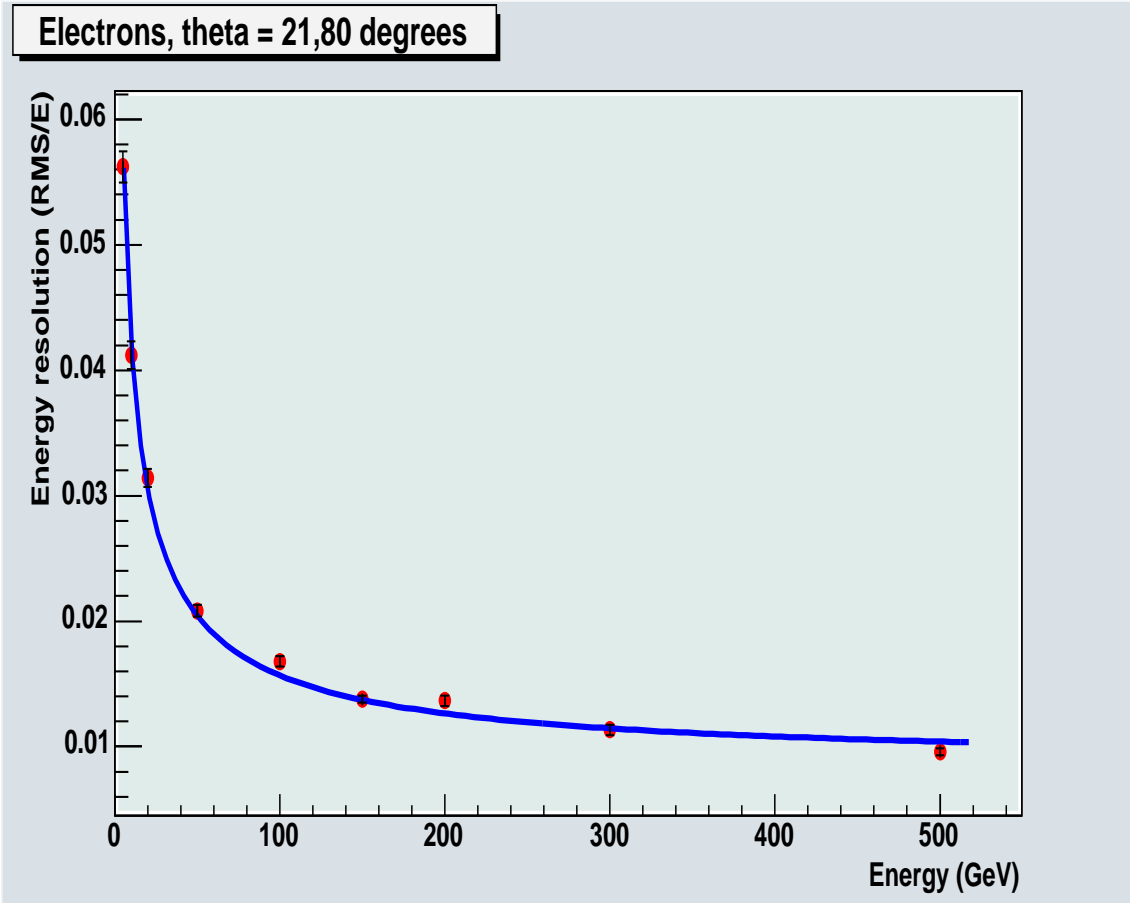


Figure 4: Energy resolution obtained from electrons of various energies in one of the end-caps of the E.M. calorimeter. The curve $a/\sqrt{E} \oplus b$ was fitted according to the method of minimization of the χ^2 (see text).

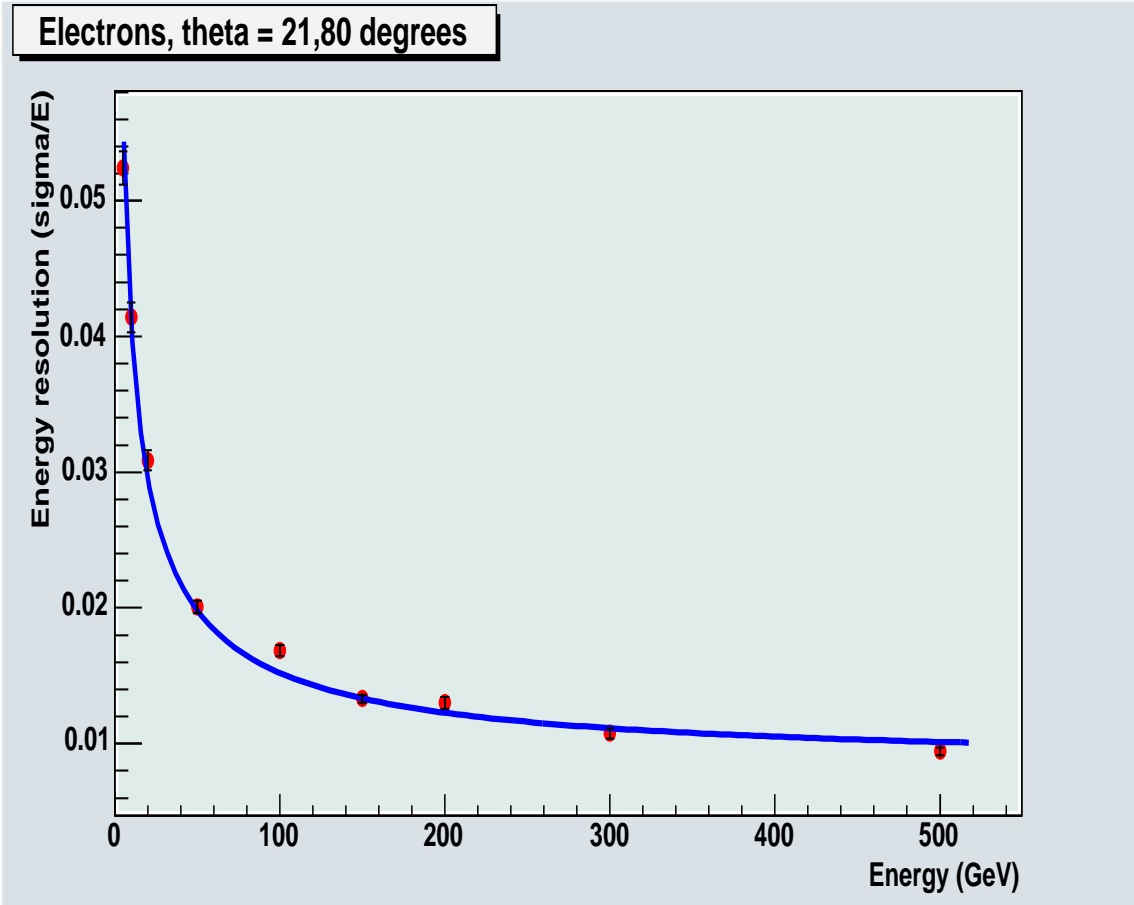


Figure 5: Energy resolution obtained from electrons in one of the end-caps of the E.M calorimeter. The curve $a/\sqrt{E} \oplus b$ was fitted according to the method of minimization of the χ^2 , (see text).

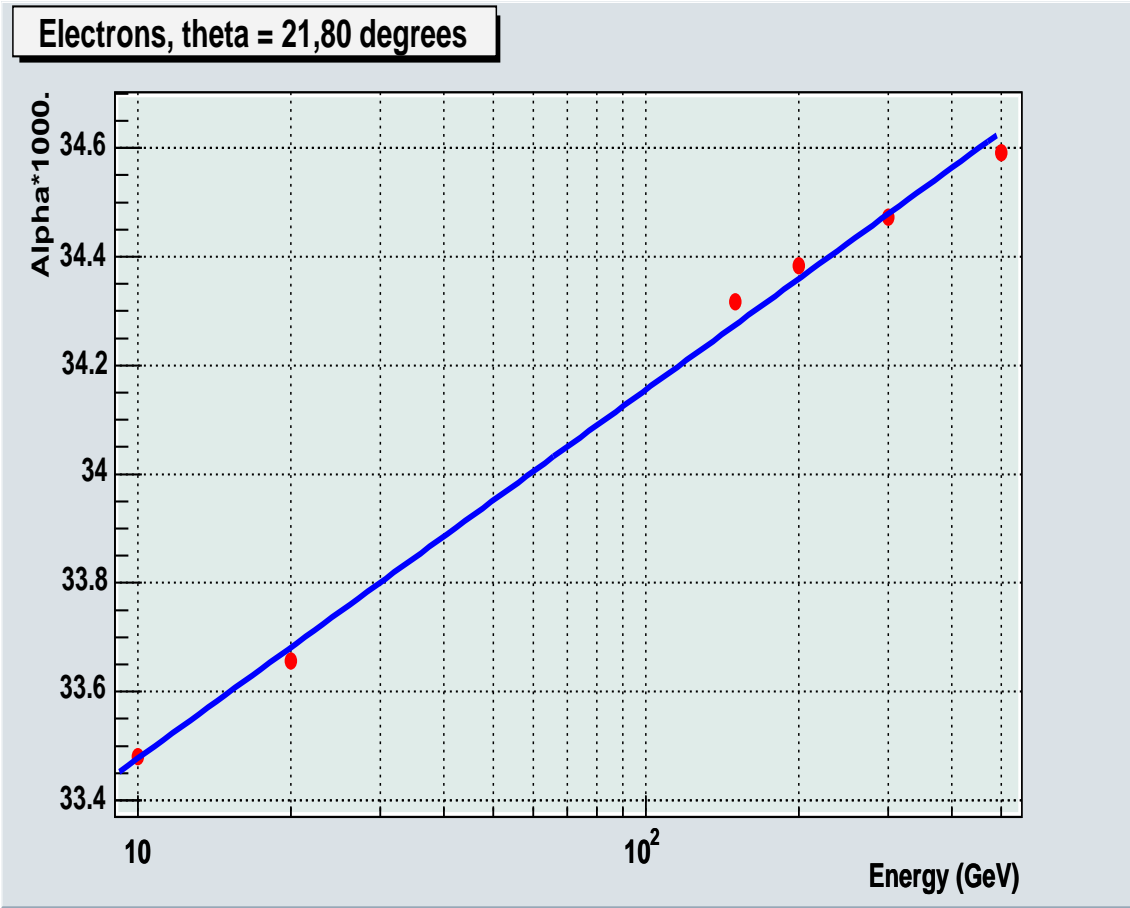


Figure 6: Variation of the parameter α according to the energy of the electrons.

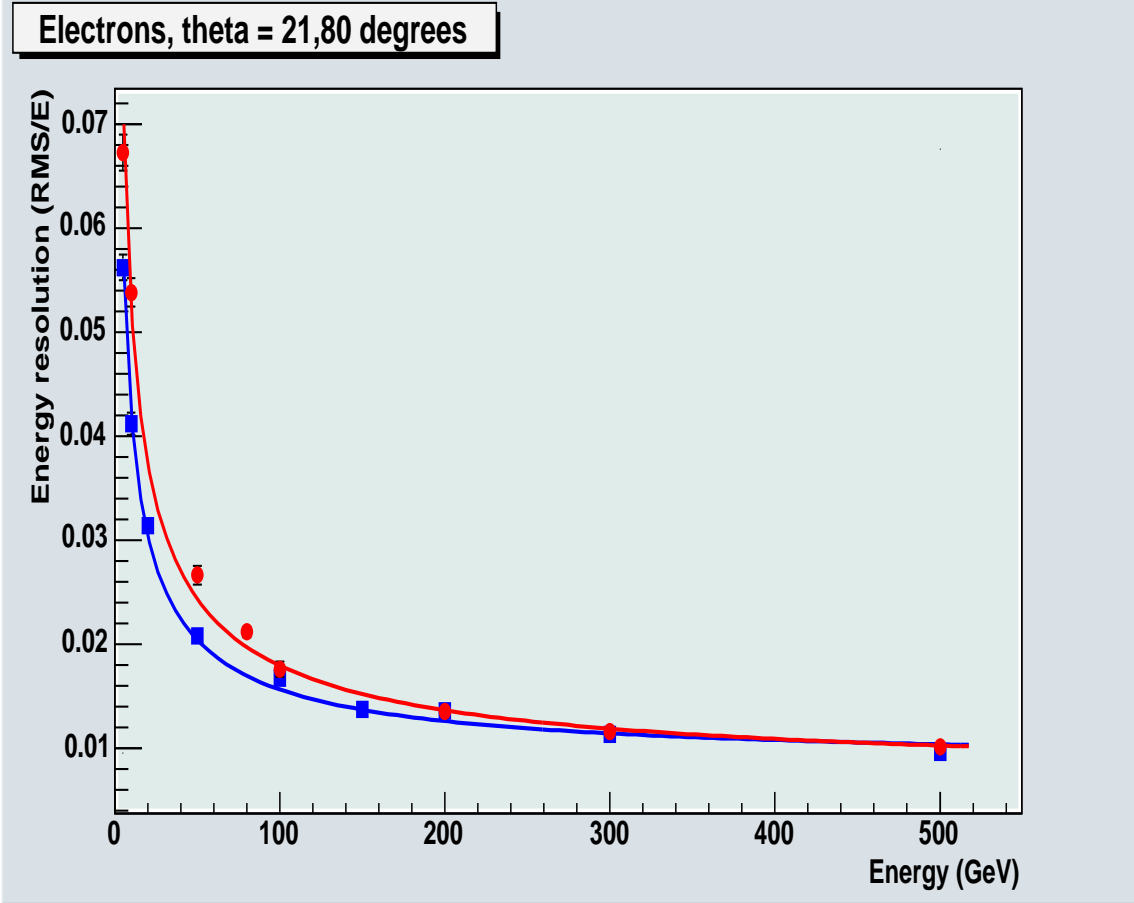


Figure 7: Energy resolution (RMS/E) according to energy E of the electrons with the E.M. calorimeter alone (blue points), and by taking of account the whole detector and the magnetic field (red points). The curves $a/\sqrt{E} \oplus b$ were fitted according to the method of minimization of the χ^2 (see text).

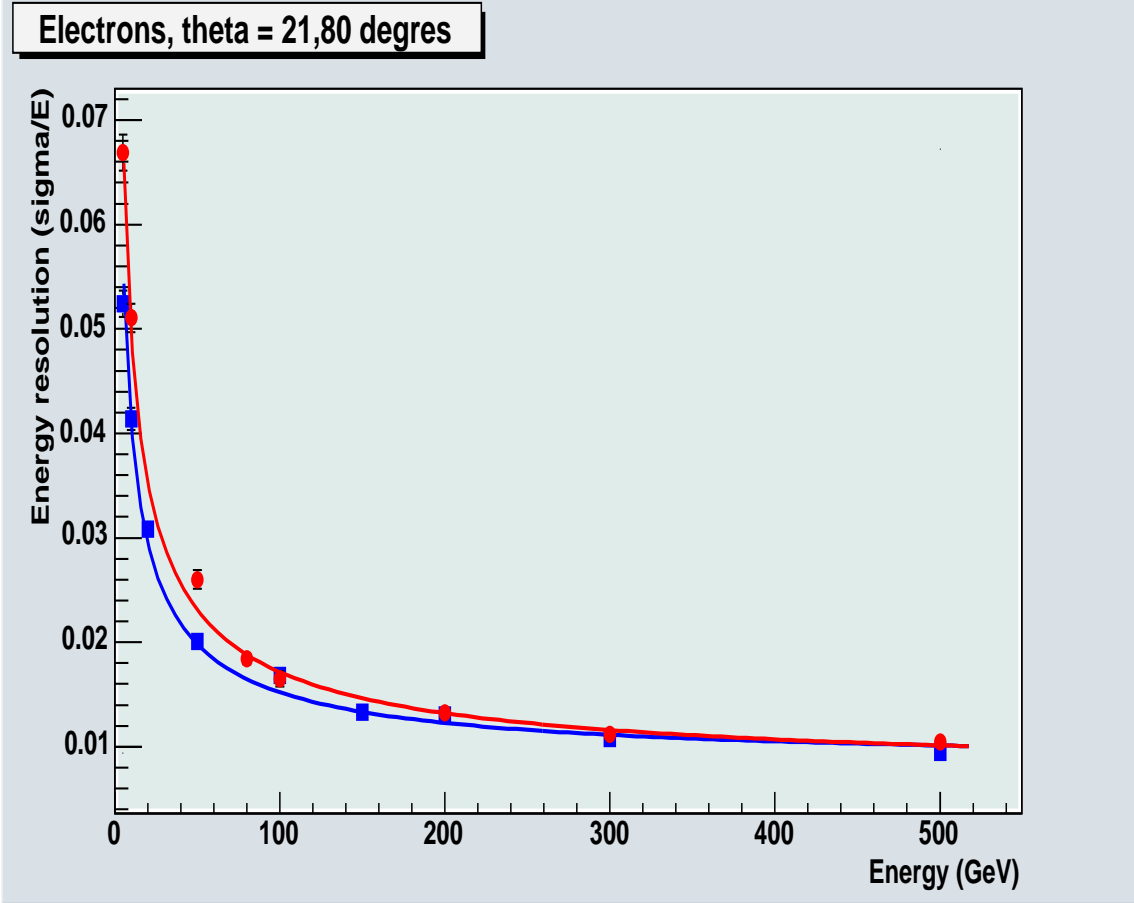


Figure 8: Energy resolution (σ_{gauss}/E) according to energy E of the electrons with the E.M. calorimeter alone (blue points), and by taking of account the whole detector and the magnetic field (red points). The curves $a/\sqrt{E} \oplus b$ were fitted according to the method of minimization of the χ^2 , (see text).

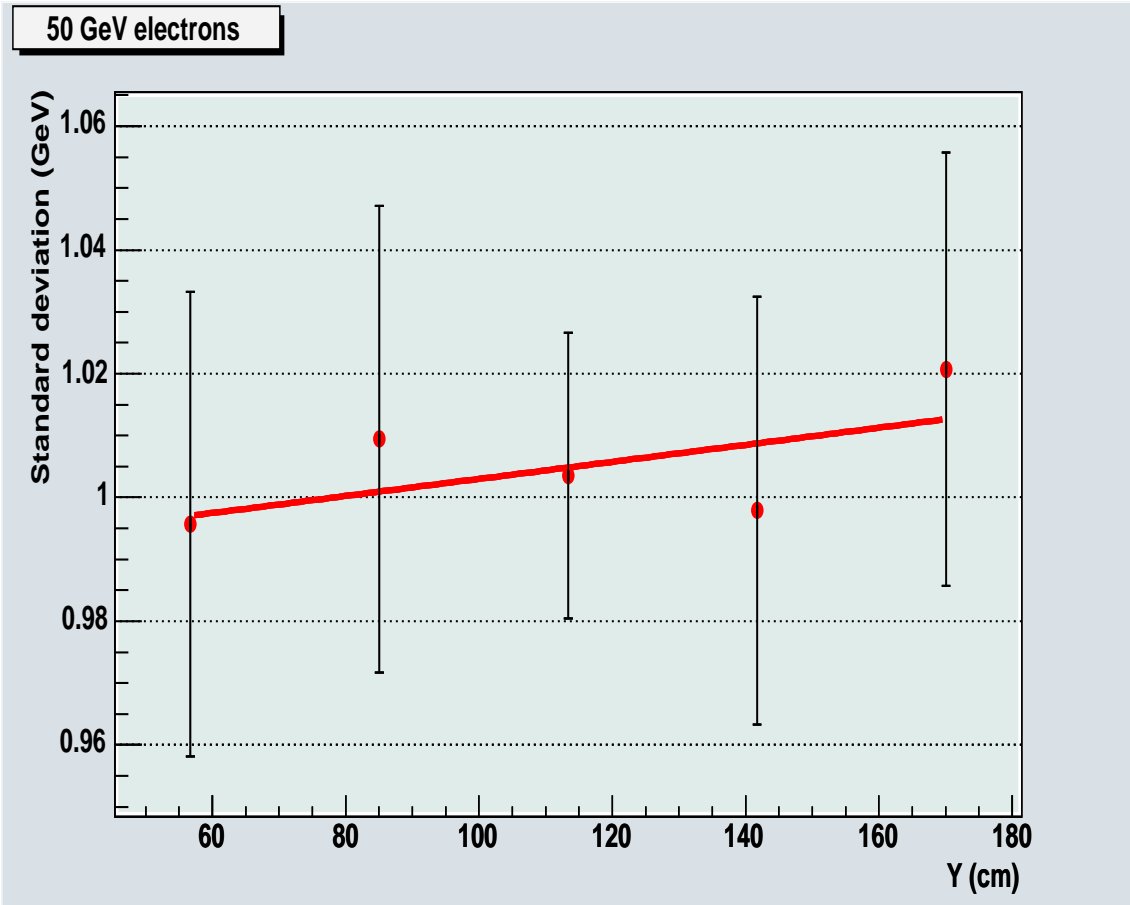


Figure 9: Standard deviation (σ_{gauss}) according to the position Y of the 50 GeV electrons in one of the two E.M. end-caps.

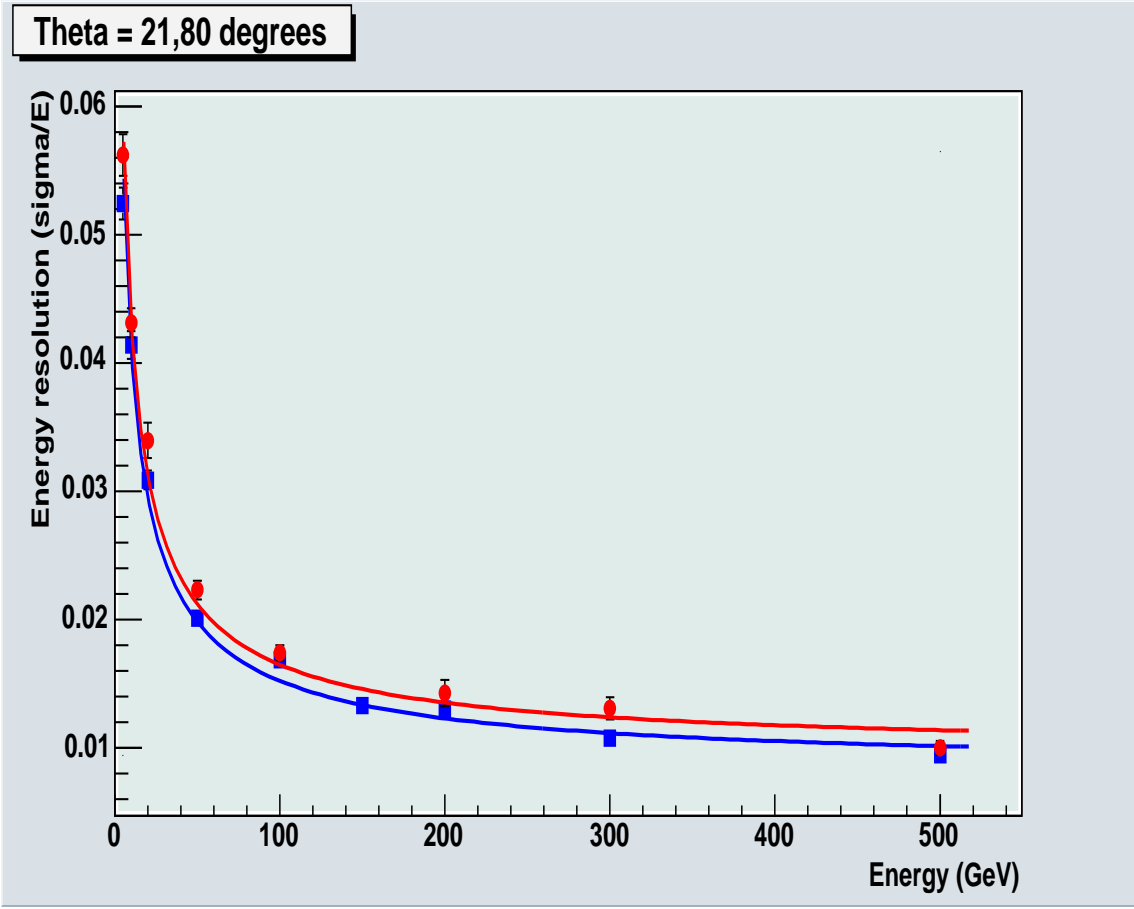


Figure 10: Energy resolution (σ_{gauss}/E) obtained with the E.M. calorimeter alone for electrons (blue points), and for photons (red points).

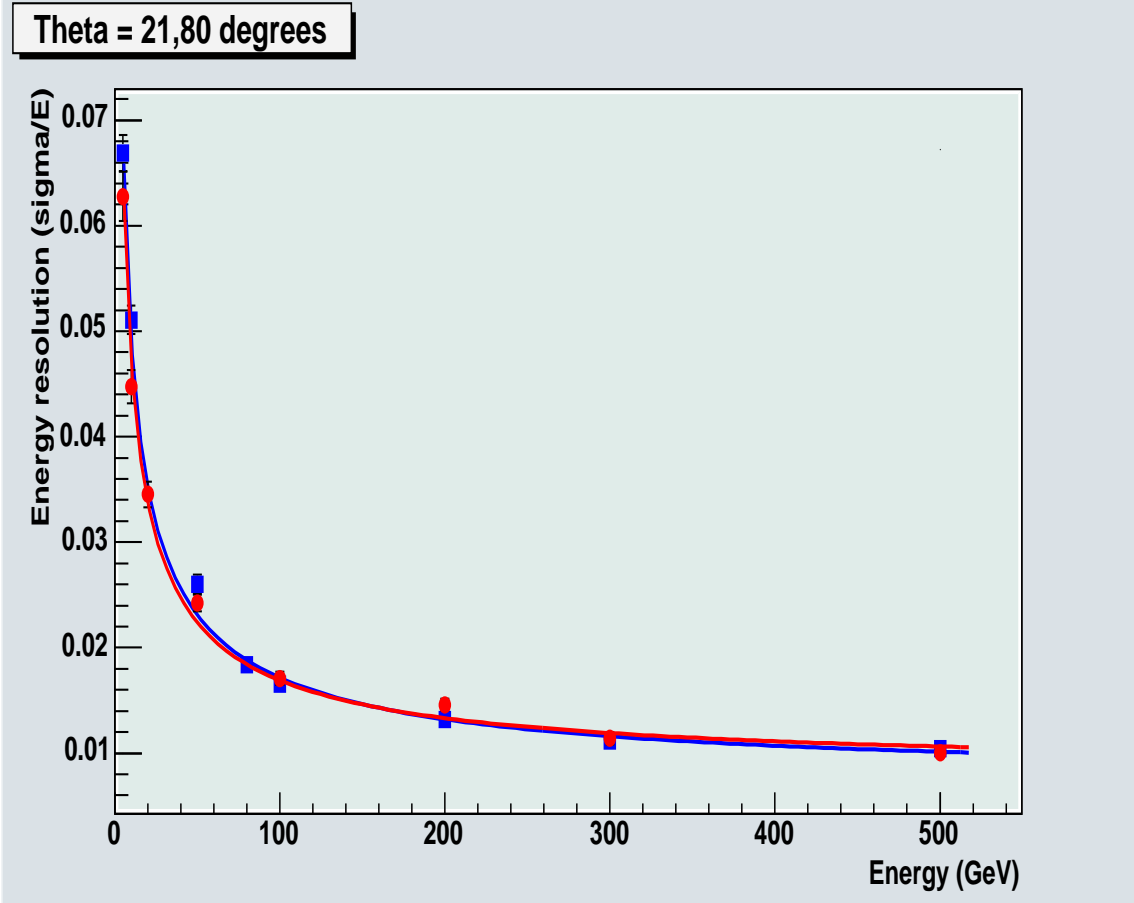


Figure 11: Energy resolution (σ_{gauss}/E) obtained with the whole detector (including the magnetic field) for electrons (blue points), and for photons (red points).